Formation of Pd-nanoparticles within the pores of ring opening metathesis polymerization-derived polymeric monoliths for use in organometallic catalysis

Rajendar Bandari,[a] Andrea Prager,[b] Thomas Höche,[b] and Michael R. Buchmeiser[a]*

[a]Lehrstuhl für Makromolekulare Stoffe und Faserchemie, Institut für Polymerchemie, Universität Stuttgart, Pfaffenwaldring 55, D-7 Stuttgart, Germany
[b]Leibniz Institut für Oberflächenmodifizierung e.V. (IOM), Permoserstraße 15, D-04318 Leipzig, Germany
E-mail: michael.buchmeiser@ipoc.uni-stuttgart.de

Dedicated to Professor Dr. Siegfried Blechert on the occasion of his 65th birthday

DOI: http://dx.doi.org/10.3998/ark.5550190.0012.406

Abstract

Polymeric monolithic supports displaying micro-, meso- and macroporosity have been prepared via ring opening metathesis polymerization (ROMP) from (Z)-9-oxabicyclo[6.1.0]non-4-ene (**OBN**) and tris(cyclooct-4-en-1-yloxy)methylsilane (**CL**) by the use of the 2nd-generation Grubbs-initiator $RuCl_2(Py)_2(IMesH_2)(CHPh)$ **1** in the presence of a phase separation-enforcing macroporogen, i.e. 2-propanol, and a microporogen, i.e. toluene. The porous supports were then subject to pore size-selective functionalization by hydrolyzing the epoxy-groups within pores >6 nm to the corresponding *vic*-diol with the aid of poly(styrenesulfonic acid) (**PS-SO_3H**). The remaining epoxide moieties located within the small pores (diameter <6 nm) were then reacted with N,N-dipyrid-2-ylamine to yield the corresponding dipyrid-2-ylamin-functionalized monolithic supports. Typical loadings with functional monomer were in the range of 6-7 μmol/g. These chelating ligands located within the small pores were then used for the immobilization of Pd^{II}. Quantitative metal loadings (approx. 1 mg/g) could be accomplished. Reduction of the Pd^{II} with $NaBH_4$ resulted in the formation of Pd nanoparticles <4 nm in diameter that were still exclusively located within the small pores. These Pd-loaded monoliths were used in a series of Sonogashira-Hagihara and Suzuki-type couplings. Scanning electron microscopy measurements on the metal loaded monoliths prior to the catalytic reactions revealed that the metal nanoparticles that formed were immobilized within the small pores. These findings are supported by the comparably low metal content in the coupling products. Thus, metal leaching was <0.13 %.

Keywords: Metathesis, monoliths, nanoparticles, ring-opening polymerization, supported catalysts, C-C coupling reactions

Introduction

Polymeric monolithic supports have evolved over the last 20 years and hold nowadays a strong position in separation science, particularly in the analysis of high molecular weight analytes as well as in downstream processing.[1-4] More recently, polymeric monolithic supports have been introduced into heterogeneous catalysis,[5-9] biocatalysis[10] and tissue engineering.[11] Within that context, the use of ring-opening metathesis polymerization (ROMP) has widened the scope and range of applications of polymeric monoliths including polymeric monoliths as catalytic supports for both batch and continuous processes.[12-26] This is related to the unprecedented tolerance versus functional groups that can be introduced onto the inner surface of the porous, cross-linked matrix. Very recently, electron beam- (EB) based synthetic protocols, allowing for the large volume synthesis of such supports, have been added to the synthetic armor.[27-30] Again, ROMP-based protocols were used for functionalization.[26]

So far, metal nanoparticles have been immobilized on microporous and mesoporous inorganic supports such as zeolithes, $Al(OH)_3$ or silica,[31-36] on polymers[37-41] or within micelles.[42, 43] Alternatively, ion exchange-based techniques have been reported for immobilization purposes.[44, 45] However, in view of the latest reports on the role of metal nanoparticles in various catalytic reactions,[46-71] we were interested whether we could permanently immobilize such nanoparticles with the confines of the small pores (<20 nm) of such a polymeric material, thereby providing a compartment for the nanoparticles that should prevent particle growth during catalysis and thus deactivation. We recently reported on the immobilization of Pd nanoparticles within the small pores of EB-triggered, free radical polymerization-derived monoliths.[72] Here, we present our latest results with ROMP-derived monolithic supports.

Results and Discussion

Monolith Synthesis

Epoxy-based monolithic columns were prepared within the confines of 4.6 x 100 mm i.d. steel columns and 20x10 mm i.d. glass cartridges (Figure 1). These monolith-filled devices can be used in a high-throughput screening set up and thus speed up screening. (Z)-9-oxabicyclo[6.1.0]non-4-ene (**OBN**) and tris(cyclooct-4-enyl-1-oxy)methylsilane (**CL**)[23] were used as monomers, 2-propanol (2-PrOH) was used as macroporogen and toluene was used as a microporogen. For monolith synthesis, **OBN** and the **CL** were dissolved in 2-PrOH. A second solution was prepared by dissolving the catalyst **1** in toluene. Both solutions were chilled to 0 °C, mixed for 30 s and the final mixture was transferred into the column (Scheme 1).

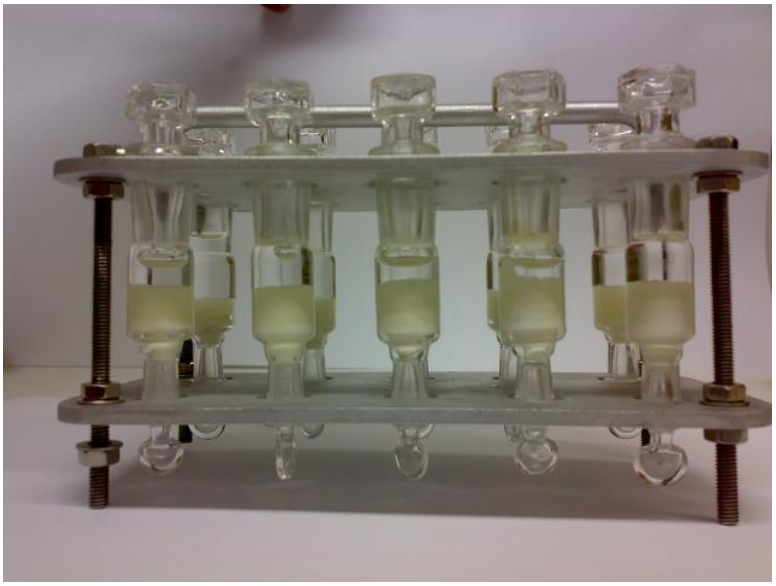

Figure 1. Monolith-filled glass cartridges (20x10 mm i.d.) for high-throughput screening.

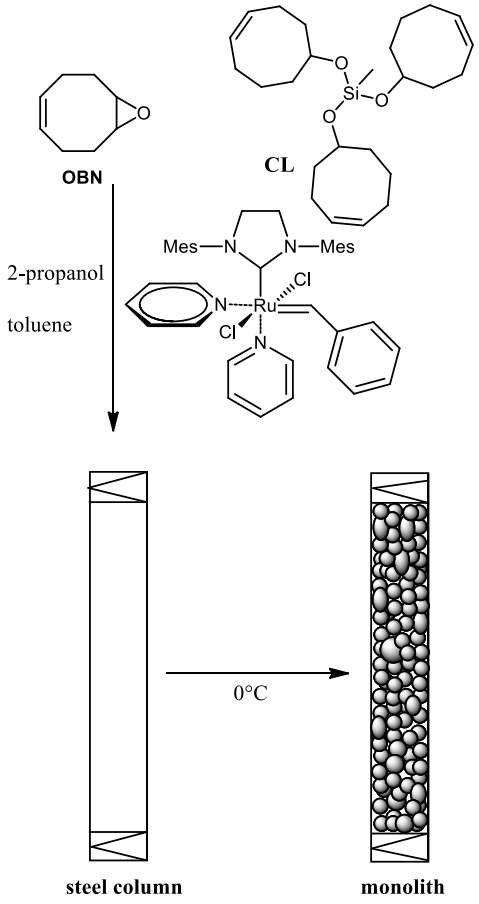

Scheme 1. Monolith synthesis.

Polymerization was allowed to proceed for 30 minutes at 0 °C, followed by 16 hours at room temperature. The columns were then cleaned, placed inside a cartridge holder and the monolith was cleaned by flushing with a solution of ethyl vinyl ether (20 wt.-%) in dimethylsulfoxide. This capping procedure ensured for an effective removal of all Ru-compounds as evidenced by ICP-OES measurements. Thus, the final Ru content in the monolithic rod was <50 ppm. After this procedure, the monoliths were ready for use and characterization, respectively.

Monolith characterization

In brief, monoliths were characterized for their inter-microglobule porosity (ε_z), micro porosity (ε_P), total porosity (ε_t), pore volume (V_p, mL/g), mean particle diameter (d_p, nm) and mean pore size (Φ_m, Å) using both inverse size-exclusion chromatography (ISEC)[73] and scanning electron microscopy (SEM). The pore volume relative to the volume fraction of the empty column, ε_p, is expressed as $\varepsilon_p=V_p/V_k$. The total porosity ε_t is the sum of both the pore porosity and interglobule porosity ($\varepsilon_t=\varepsilon_p+\varepsilon_z$). The mean pore size Φ_m of the monoliths was calculated from the graph of log Φ_{av} (Å) *vs.* ΔR (%). A summary of the monolith's structures in terms of volume fraction of pores, volume fraction of inter microglobule void volume, total porosity, pore volumes, mean pore size, and pore size distribution is provided in Table 1 and Figure 2, respectively. Measurements of the pore size distribution revealed that 70% of the pores were <20 nm and 60% of the pores were even <2 nm (Figure 2).

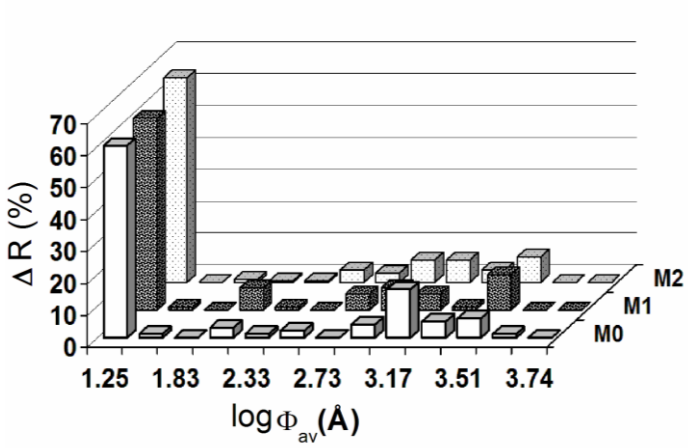

Figure 2. log$\Phi_{average}$ (Å) *vs.* ΔR (%) for the unmodified (**M0**), the **PS-SO$_3$H**-modified **(M1**), and the dipyrid-2-ylamine modified monolith **(M2**).

The monoliths were then further characterized by scanning electron microscopy (SEM). SEM provides a robust picture of the monolithic structure, the size and three-dimensional form of the structure-forming micro-globules as well as of the macropores, which are usually in the micrometer range. An illustrative SEM picture of cross sections of a monolith prepared according to the recipe shown in Table 1 is shown in Figure 3. One can clearly see the macroporous structure and the structure-forming microglobules with average diameters in the sub-micrometer range.

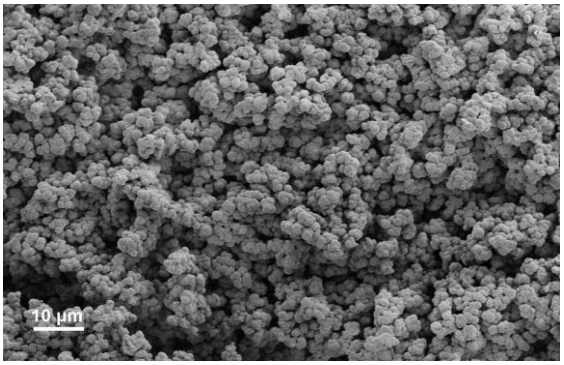

Figure 3. Structure of unmodified monoliths.

Table 1. Composition and structural data of monoliths

Composition (wt.-%)				
OBN	CL	2-PrOH	toluene	catalyst
20	20	50	10	0.2
Structural data (before modification)				
ε_p (vol-%)	ε_z (vol-%)	ε_t (vol-%)	V_p (µl/g)	Φ_m (Å)
20	50	70	528	622
Structural data (after hydrolysis of parts of the epoxide groups with PS-SO_3H)				
20	47	68	531	555
Structural data (after functionalization with dipyrid-2-ylamine)				
20	46	66	512	548

Pore-size specific functionalization of monoliths

The concept of pore size-specific modification with polymeric monoliths introduce for separation issues by Svec and Fréchet some 15 years ago.[74] Applying the same principle, we aimed on the generation of nanoparticles of defined particle size that were synthesized within the confines of suitable functionalized small pores for use in catalytic reactions. In brief, the concept of the pore size-selective functionalization entails the use of a polymeric reagent that hydrolysis the epoxy groups inside pores that can be penetrated by this reagent, while leaving the epoxy groups in small pores unaffected. The latter can then be reacted with a suitable nucleophilic reagent, e.g., an amine, to selectively functionalize these small pores. The resulting monolithic material thus finally contains pores with different surfaces functionalities.

From ISEC measurements, it is obvious that the monoliths contained pores <20 and >20 nm. For hydrolysis of the epoxy-groups within pores >20 nm, we choose an aqueous 1 wt.-% solution of poly(styrenesulfonic acid) (**PS-SO_3H**) with an M_w of 2600 g·mol^{-1} and a narrow molecular weight distribution (PDI =1.01). **PS-SO_3H** with such a molecular weight has a hydrodynamic diameter of roughly 7 nm. As a rule of thumb, a polymer can enter a (cylindrical) pore, whose diameter is about 2.5 times larger than its mean square radius of gyration. Consequently, all epoxide groups in pores

>20 nm become hydrolyzed. In a second step, the remaining epoxide groups located in smaller pores (<20 nm) were then reacted with a 10 wt.-% solution of N,N-dipyrid-2-ylamine in CH_2Cl_2. Scheme 2A and Scheme 2B illustrate the process. Typical loadings with N,N-dipyrid-2-ylamine as determined by elemental analysis were in the range of 6-7 micro-mol/g polymer.

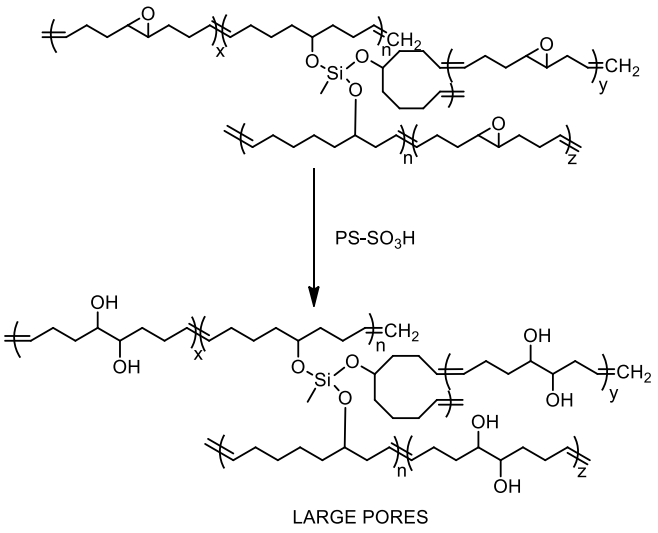

Scheme 2A. Pore size-selective hydrolysis of the epoxy groups with pores >20 nm.

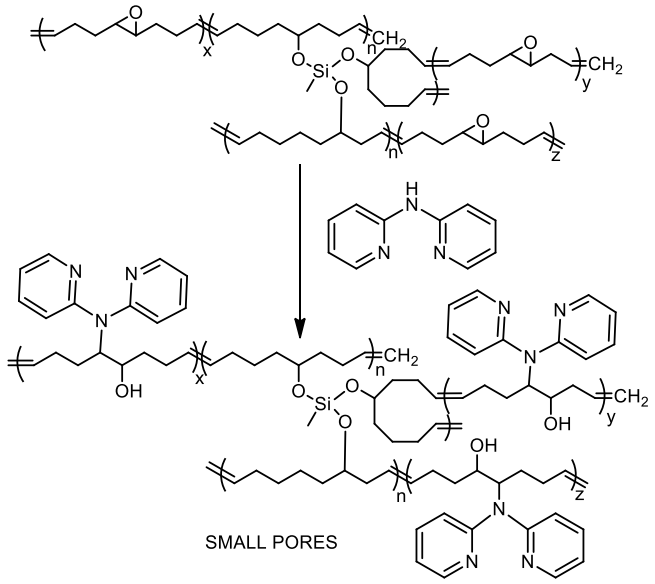

Scheme 2B. Pore size-selective functionalization of pores <20 nm.

For purposes of comparison, a thus functionalized monolith was again characterized by ISEC. No significant difference in the volume fraction of pores of the monolith was observed, (ε_p=20%), however the total porosity ε_t slightly decreased from 68 to 66% (Table 1). This increase may well be explained by the loss of void volume during functional monomer immobilization.

Immobilization of Pd^{II} within dipyrid-2-ylamine-functionalized pores

An aqueous solution of H_2PdCl_4 was pumped through the *N*,*N*-dipyrid-2-ylamine-functionalized monolith. After extensive washing, the final Pd-loading was determined by ICP-OES and was found to be 1 mg of Pd/g of monolith. From this Pd^{II} bound to the dipyrid-2-ylamine ligand, Pd-nanoparticles were generated via reduction with an aqueous 10 wt.-% solution of $NaBH_4$. The nanoparticles that formed within pores <20 nm were approximately 4 nm (Table S1 and Figure S1; Supporting Information) in diameter. The presence of Pd-metal was confirmed by energy dispersive X-ray spectrometry (EDXS) and ICP-OES measurements (Figure 5). Finally, the thus prepared Pd(0)-loaded monoliths were used as catalysts for various Pd-mediated cross-coupling reactions such as for Suzuki- and Cu-free Sonogashira-Hagihara-type couplings. Scheme 3 illustrates the process of nanoparticle formation within the small pores. Figure 4a gives an illustration of the Pd nanoparticles that were generated.

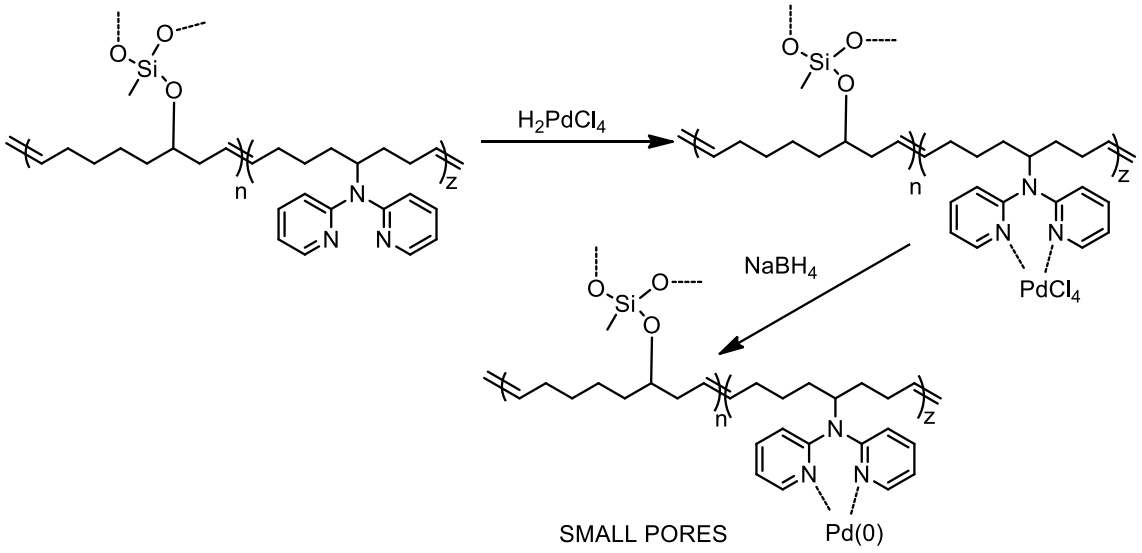

Scheme 3. Metal loading of dipyrid-2-ylamine-functionalized small pores. Reduction of Pd^{II} by $NaBH_4$ leads to Pd-nanoparticles immobilized within small pores.

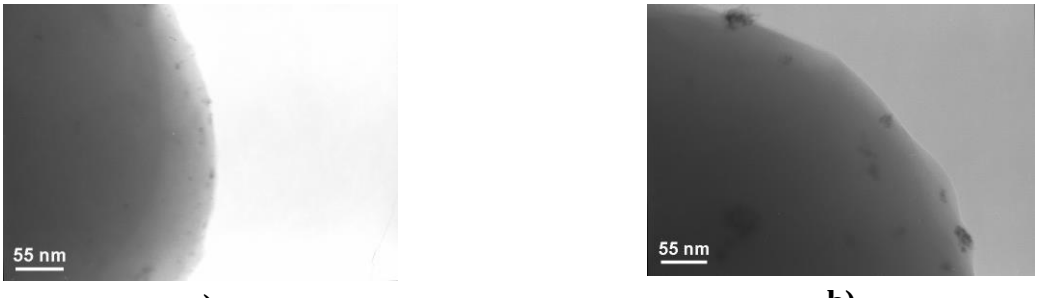

a) **b)**

Figure 4. TEM micrographs of Pd immobilized on the monolithic supports, a) before and b) after use in C-C coupling reactions.

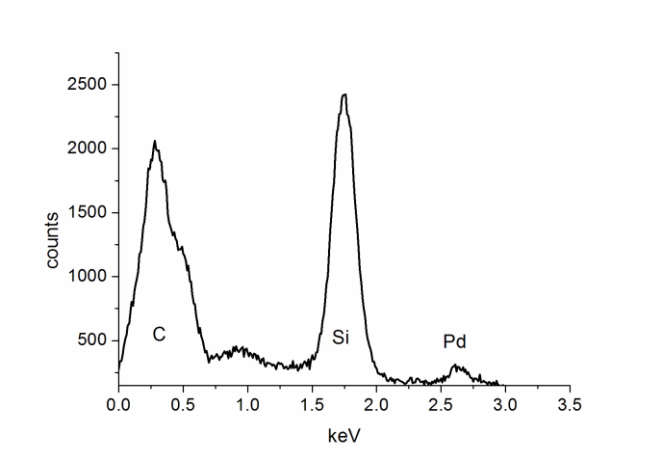

Figure 5. EDX spectrum of Pd nanoparticles formed within the small pores of a monolith.

Application of monolith-supported Pd nanoparticles in cross-coupling reactions

Suzuki-type cross-couplings. First, the Suzuki-type cross-coupling reaction between bromo- or chlorobenzene and phenyl boronic acid in water and in the presence of monolith-supported Pd^0 (Scheme 4) was studied. All catalytic reactions were carried out in monolithic discs (Figure 1) at 50 °C. The use of such discs allows for a high-throughput setup, thereby speeding up the screening process.

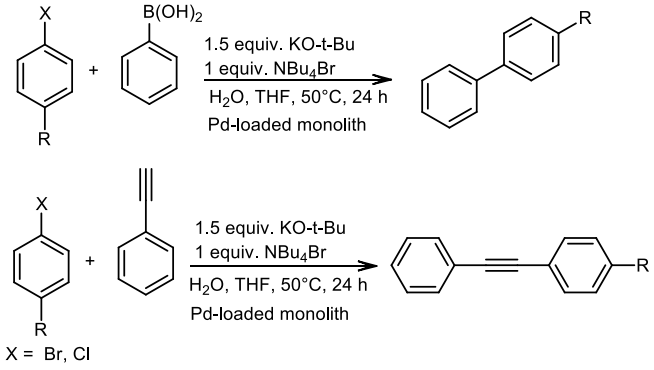

Scheme 4. Suzuki- and Sonogashira-Hagihara-type cross couplings catalyzed by monolith-supported Pd-nanoparticles.

Monolithic polymeric discs (~150 mg) with a Pd-loading of 1.4 μmol were used. Using a series of activated and deactivated aryl bromides, the desired coupling products formed with turn-over numbers (TONs) up to 2900 with respect to the number of palladium surface atoms present in all palladium nanoparticles (Table 2). Significant homocoupling (up to 18%) was observed with *m*- and *p*-NO_2-bromobenzene. As anticipated, substitution in the *o*–positions resulted in reduced yields and TONs due to steric hindrance as compared to the *p*-substituted benzenes.

Table 2. Pd nanoparticle-catalyzed Suzuki-type-cross-coupling reactions with phenylboronic acid. Yields were determined by GC using t-butylbenzene as internal standard, hcp=homocoupling product (biphenyl). Values in brackets represent the data obtained after reuse

#	Halide	Product	Product yield (%)	Yield of hcp[a] (%)	TON[b]
1	C_6H_5Br	biphenyl	60 (58)	0 (0)	1760 (1660)
2	4-Br-trifluromethyl-benzene	4-trifluoro-methylbiphenyl	87 (89)	1 (1)	2560 (2590)
3	pentafluoro-bromobenzene	2,3,4,5,6-pentafluoro-biphenyl	43	9	1530
4	4-NO_2-bromobenzene	4-NO_2-biphenyl	84	16	2940
5	3-NO_2-bromobenzene	3-NO_2-biphenyl	87 (86)	11 (11)	2880 (2770)
6	2-NO_2-bromobenzene	2-NO_2-biphenyl	80	18	2880
7	C_6H_5Cl	biphenyl	5	0	150
8	4-methoxy-bromobenzene	4-methoxy-biphenyl	36	6	1230

[a]hcp=homocoupling product (biphenyl derivative).
[b]Assuming that only the surface palladium atoms participate in the reaction.

To check for the size-stability of the nanoparticles, which directly affects their catalytic activity, a Pd-loaded monolith was reused for the coupling of bromobenzene, 1-bromo-4-(trifluoromethyl)benzene and 1-bromo-3-nitrobenzene, respectively. No noticeable change in conversion was observed (entries 1, 2 and 5, Table 2). However, there was a significant change in

the average diameter of the Pd nanoparticles from 4 nm to 16 nm as observed by SEM (Figure 4b, (Figure S2, Supporting Information). This suggests that almost any Pd-species in an oxidation state different from zero [i.e. Pd(II) or Pd(IV)][52, 75, 76] that is formed finally re-enters the nanoparticle as Pd(0) presumably via Ostwald ripening. The nanoparticles, however, mostly remain inside the pores <20 nm. Consequently, the Pd-leaching as determined by ICP-OES was very low. Thus, only 0.13 % of the Pd originally present within the monolith leached into the reaction mixture.

Sonogashira-Hagihara-type cross-couplings. The monolith-supported Pd-catalysts were also used in Cu-free Sonogashira-Hagihara-type cross-coupling reactions. Using iodobenzene as well as a series of activated and deactivated bromobenzenes, TONs up to 4130 were obtained assuming that only the surface Pd-atoms participate in the reaction.

Table 3. Pd-nanoparticle-catalyzed, Cu-free Sonogashira-Hagihara-coupling reactions of different halides with ethynylbenzene. Yields were determined by GC-MS using *t*-butylbenzene as internal standard

#	Halide	Product	Product yield (%)	TON[a]
1	C_6H_5Br	tolan	10	430
2	4-NO_2-bromobenzene	4-NO_2-tolan	36	1560
3	4-methylbromobenzene	4-methyltolan	5	220
4	4-methoxybromobenzene	4-methoxytolan	2	90
5	C_6H_5I	2,4,6-trimethyltolan[b]	95	4130

[a]Assuming that only the surface palladium atoms participate in the reaction. [b]mesitylethyne was used.

A comparison of the catalytic data obtained with the ROMP-derived monolithic supports presented here with those obtained with Pd-nanoparticles immobilized on acrylate-derived monolithic supports[72] reveals some differences. Thus, the TONs obtained in the Pd-mediated Suzuki-type cross-coupling reactions are by far higher with Pd-loaded acrylate-derived monolithic supports than with the ROMP-derived support. At a first glance, this is somewhat surprising since the same methodology, i.e. a pore-size selective functionalization approach was used for the

generation and immobilization of the Pd nanoparticles. However, a closer look at the structural differences of these two types of monolithic supports reveals some differences. While the ROMP-derived supports have a higher relative abundance of very small pores (>60% are smaller than 2 nm in the modified monolith), these supports have very few pores in the range of 2-20 nm. In contrast, approx. 12% of the pores in acrylate-derived monoliths possess a pores size of approx. 4 nm. Upon reaction with Pd(II) and reduction with $NaBH_4$, Pd-nanoparticles approx. 2 nm in diameter are formed in the pores of the acrylate-derived supports. These remain size-stable throughout the catalytic reaction and give raise to high TONs.[72] Due to the very low fraction of pores in the 2-20 nm region, this is apparently not possible with the ROMP-derived supports. This is also reflected by the lower Pd-loadings that can be achieved (approx. 30% of the Pd loading achieved with ROMP-derived monoliths as compared to acrylate-derived monoliths). During catalysis, Ostwald ripening occurs and larger Pd-particles form, whose catalytic activity rapidly decreases with increasing size. Consequently, supports with a large volume fraction of pores in the 3-4 nm region must be considered to be best suited for ligand-free catalytic reactions.

Experimental Section

General. $[RuCl_2(PCy_3)(IMesH_2)(CHPh)]$ ($IMesH_2$=1,3-bis(2,4,6-trimethylphenyl)-4,5-dihydroimidazol-2-ylidene), (PCy_3=tricyclohexylphosphine), *m*-chloroperbenzoic acid, $LiAlH_4$, 1,5-cyclooctadiene, *cis*-cyclooctene, ethyl vinyl ether (EVE) and the 0.01 mol L^{-1} standard NaOH solution in methanol as well as dimethylsulfoxide (DMSO) were obtained from Aldrich Chemical Co. (Germany) and used as received. $[RuCl_2(pyridine)_2(IMesH_2)(CHPh)]$ **1**[23], (Z)-9-oxabicyclo[6.1.0]non-4-ene (**OBN**)[23], tris(cyclooct-4-en-1-yloxy)methylsilane (**CL**)[23] were prepared according to the literature. Triethylamine (Fluka, Switzerland) was dried over CaH_2 and distilled prior to use. Narrow polystyrene (PS) standards with molecular masses (M_w) of 972, 2600, 4000, 6810, 17200, 30000, 200000, 400000, 803000, 3390000 and 4110000 g/mol were purchased from Waters Inc. (USA) and PSS (Pittsburgh, PA, USA). Chloroform (99.5%) and 2-propanol were purchased from Acros Laborchemie Handels GmbH (Germany), and dried over CaH_2 prior to use. Toluene and CH_2Cl_2 were dried by an MBraun SPS solvent purification system. For GPC and inverse ISEC,[77] an L-4500 UV detector (Merck), and an L-6200A HPLC pump (Merck) equipped with a manual sample injection system were used. A D-7000 HPLC system was used for data acquisition and processing. ICP-OES measurements were carried out on a Spectro Ciros Vison (Spectro Analytical Instruments GmbH&Co, Germany). An MLS 1200 mega was used for the microwave-assisted dissolution of the polymeric samples. Programming: 20-180 °C within 15 min, 15 min at 180 °C, then to 20 °C within 1 h. For EDX measurements, a Bruker Axs Quant ax-EDX Microanalysis-System (Bruker Axs Microanalysis GmbH, Germany) combined with an Ultra 55 SEM (Carl Zeiss SMT, Oberkochen, Germany) was used. Conditions for EDX measurements: -10 kV, working distance 9 mm, tilt: 30 – 45 ° (depending on the sample), counting rate: ca. 1000 cps, magnification: 10000. NMR data were obtained at 250.13 MHz for proton and at 62.90 MHz for carbon in the indicated solvent at 25 °C on a Bruker Spectrospin 250 and are listed in parts per

million downfield from tetramethyl silane for proton and carbon. IR spectra were recorded on a Bruker Vector 22 using ATR technology. GC-MS investigations were carried out on a Shimadzu GCMS QP5050, using a SPB-5 fused silica column (30 m x 0.25 µm film thickness).

General procedure for the preparation of monoliths

Monoliths were prepared as follows. Stainless steel columns (150 x 4.6 mm i.d.) were cleaned, rinsed and sonicated in a 1:1 mixture of ethanol and acetone. Glass cartridges (20 x 10 mm i.d.) were cleaned as described earlier[78]. The columns were then dried for 2 h under vacuum, then closed at one end with frits and end fittings, respectively, and cooled to 0 °C. Separately, two different solutions (**A**, **B**) were prepared and cooled to 0 °C. Solution A consisted of 20 wt.-% of (**OBN**, 20 wt.-% of **CL**, and 50 wt.-% of 2-propanol, while solution B consisted of a solution of **1** (0.2 wt-%) in 10 wt.% of toluene. Both solutions were merged at 0°C and mixed for 30 s. The column was filled with the polymerization mixture, sealed with Teflon caps and kept at 0 °C for 30 minutes. After rod formation was finished, the column was removed from the ice bath and stored at room temperature for 16 h. In order to remove initiator and excess of **OBN** and **CL**, the column was provided with new frits and flushed with a mixture of EVE (20 vol.-%) in DMSO for 2 hours at a flow rate of 0.3 mL/min. Finally, it was flushed with $CHCl_3$ for 1 h at a flow rate of 0.3 mL/min. Monolithic discs were washed with 10 mL of 20 vol.-% EVE in DMSO.

Preparation of disks. Glass discs (20 x 10 mm i.d.) were cleaned as described earlier. The disks were then dried for 2 h under vacuum, closed at one end with a glass stopper, and cooled to 0 °C. Separately, two different solutions (**A**, **B**) were prepared (*vide supra*) and cooled to 0 °C. Both solutions were merged at 0 °C and mixed for 30 s. The disks were filled with the polymerization mixture by using a 5 mL syringe, sealed with another stopper and kept at 0 °C for 30 minutes. After rod formation was finished, the disks were removed from the ice bath and stored at room temperature for 16 h. Then, the two stoppers were removed from both ends, the discs were mounted to a filtration device and slowly washed with 10 mL of a solution of EVE (20 vol.-%) in DMSO. Finally, the disks were washed with 5 mL of $CHCl_3$.

Pore size-selective modification. In a first step, the epoxy groups within large pores (>20 nm) of the porous polymer rod were hydrolyzed by flushing the monolithic column/disc with an aqueous solution of **PS-SO$_3$H** (M_w ~2600 g/mol) for 15 min at a flow rate 0.3 mL/min. For that purpose, a 1 wt.-% solution of **PS-SO$_3$H** was prepared from 200 mg of the polymer dissolved in 18 mL of water and 2 mL of THF. Finally, the monolith was kept for 15 h at 65 °C. The monolith-containing column was then attached to an HPLC pump and washed for 2 h at a flow rate of 0.3 mL/min with water/THF (80:20 vol.-%) and then with THF for 1 hour. These columns were then characterized by ISEC. The discs were subsequently washed with a THF:water mixture (20:80 vol.-%), then with 5 mL of THF and finally with 5 mL of CH_2Cl_2.

The epoxide groups within the small pores were reacted with 2,2´-dipyridylamine by injecting a solution of 2,2´-dipyridylamine (1.0 g dissolved in 10 mL of CH_2Cl_2) and heating the column to 40 °C for 18 h. The thus modified column was again attached to the HPLC and washed successively with 50 mL of CH_2Cl_2 (flow rate 0.3 mL/min). The final effluent was free of 2,2'-dipyridylamine as checked by GC-MS.

Monolith characterization by ISEC. After synthesis, monolithic columns were characterized by ISEC[77] in terms of intermicroglobule porosity (ε_z), microporosity (ε_P), total porosity (ε_t), pore volume (V_p, mL/g) and mean pore diameter (Φ_m, Å). 10 µL samples of individual PS standards (0.25 mg/mL) dissolved in the mobile phase ($CHCl_3$) were injected onto each column applying a flow rate of 0.6 mL/min. For the determination of the total accessible porosity of the column, a 10 µL of sample benzene was injected. All the chromatograms were recorded at a wavelength of 254 nm. Retention times and volumes corresponding to each injection were determined from the peak maximum. All retention volumes were corrected for the extra-column volume of the equipment. Calculations were carried out by assuming that the hydrodynamic radii of the PS standards in $CHCl_3$ do not differ significantly from those reported in CH_2Cl_2. Similarly, measurements were carried out after pore size selective functionalization.

Preparation of Pd-loaded monoliths. H_2PdCl_4 was prepared from anhydrous $PdCl_2$ (25 mg, 0.14 mmol), HCl (37 wt.-% solution); and NaOH (15 wt.-% solution) as described earlier.[79] A solution of H_2PdCl_4 (2.5 mL) was introduced into the N,N-dipyrid-2-ylamine-derivatized monolith. After 2 minutes, washing was carried out using 20 mL of a water:THF mixture (80:20 vol.-%). Finally, the support was dried under vacuum for 4 h. The Pd-content was measured by ICP-OES.

Determination of Pd loading. 30-40 mg samples of the monoliths were dissolved in a minimum amount of *aqua regia* (typically 5-7 mL) applying microwave irradiation. The digest was transferred into a volumetric flask and the volume of the solution was adjusted to 10.000 mL. Pd was measured at λ=340.458 nm, the back ground was measured at λ_1=340.458 and λ_2=360.955 nm. The limit of detection (LOD) was 0.014 mg/L. For calibration, Pd-containing aqueous standards (pH=1, nitric acid) with Pd concentrations of 0, 0.004, 0.14, 0.5, and 12.0 mg/L were used. Ru was measured at λ=267.759 nm, the background was measured at λ_1=267.759 and λ_2=240.998 nm, respectively. The limit of detection (LOD) was 0.008 mg/L. For calibration, Ru-containing aqueous standards (pH=1, nitric acid) with Ru concentrations of 0, 0.004, 0.14, 0.15, and 12 mg/L were used.

Suzuki-type cross-coupling. Phenylboronic acid (80 mg, 0.662 mmol), the aryl halide, e.g., bromobenzene (104 mg, 0.662 mmol), and KO-*t*-Bu (120 mg, 0.991 mmol) were added to a mixture of distilled water (2 mL) and THF (2 mL). NBu_4Br (212 mg, 0.661 mmol) and *t*-butylbenzene (36.0 mg, internal standard) were added and the mixture was stirred for 30 min. A 2 mL aliquot was filled into a monolith-filled glass cartridge, which was then sealed with glass stoppers and kept at 50 °C for 24 h. Then, the mixture was removed from the monolith, diluted with water and all organic products were extracted with 6 mL of diethyl ether. Conversion was checked by GC-MS.

Sonogashira-type-coupling. Phenylacetylene (100 mg, 0.980 mmol), *t*-butyl benzene (36 mg, internal standard), an aryl halide, e.g., bromobenzene (153 mg, 0.980 mmol), and KO-*t*-Bu (180 mg, 1.47 mmol) were dissolved in a mixture of distilled water (2 mL) and THF (2 mL). NBu_4Br (323 mg, 0.98 mmol) was added and the mixture was stirred for 5 min. Then a 2 mL aliquot was added to the monolith-filled glass cartridge, which was then sealed with glass stoppers and kept at 80 °C for 24 h. The organic products were extracted with 6 mL of diethyl ether. Conversion was checked by GC-MS.

Preparation of PS-SO_3H[80] PS (2.0 g, M_w~ 2600 g·mol^{-1}) were dissolved in 25 mL of CH_2Cl_2. Then, the solution was heated to 40 °C. 10 mL of a freshly prepared acetyl sulfate solution were added and the solution became light yellow. The reaction mixture was stirred at 40 °C for 2 h, then the reaction was terminated by adding an excess of 2-propanol over a period of 30 min and the mixture was cooled to room temperature. The CH_2Cl_2 was then removed under vacuum. The sulfonated polymer was isolated by precipitation. For this purpose, the reaction mixture was slowly added 100 mL of boiling water. The precipitate was filtered off and washed several times with water. The residue white solid was then dried under vacuum and stored in a desiccator. Yield 1.5 g (78 %). IR (cm^{-1}): 3434 (b), 3032 (m), 3059 (m), 3024 (m), 2920 (s), 2848 (m), 2932 (m), 1758 (s), 1636 (s), 1599 (s), 1451 (s), 1410 (m), 1170 (b), 1127 (s, -SO_3H), 1035 (s, -SO_3H), 1006 (s), 921 (s), 874 (m), 832 (m), 776 (s), 698 (m), 672 (m). ^1H NMR (250.13 MHz, $CDCl_3$): δ_H 11.21 and 10.08 (s, 1H), 6.55-7.56 (b, 4H), 0.66-1.45 (b, 3H). ^{13}C NMR (250.13 MHz, $CDCl_3$): δ_C 145.8, 136.9, 128.5, 128.0, 126.3, 40.9, 33.7, 24.5.

Determination of the degree of sulfonation. The degree of sulfonation of **PS-SO_3H** was determined by titration with a 0.01 mol L^{-1} standard NaOH solution in methanol (f=1.000). Titrations were carried out by dissolving 50 mg of PS-SO_3H in 5 mL of methanol. A degree of sulfonation of 70 mol.-% was found.

Conclusions

In summary, we have adapted the concept of pore size-selective functionalization to the synthesis of metal nanoparticles immobilized within the confines of the pores of ROMP-derived polymeric monolithic supports. These have been used in formats applicable to high-throughput screening, i.e. as monolithic discs inside glass columns. Using this format, the Pd-loaded monolithic supports have successfully been used in Pd-mediated coupling reactions. These Pd-loaded supports can be reused and allow for the synthesis of the desired coupling products with low Pd-contaminations (<40 ppm).

Acknowledgements

This work was supported by a grant provided by the *DFG* (*Deutsche Forschungsgemeinschaft*, grant no. BU 2174/1-2), the *Freistaat Sachsen* and the *Federal Government of Germany*.

References

1. Švec, F.; Tennikova, T. B.; Deyl, Z. *Monolithic Materials: Preparation, Properties and Application*. Elsevier: Amsterdam, 2003; Vol. 67, p 1.
2. Buchmeiser, M. R. *Polymer* **2007**, *48*, 2187.
3. Jungbauer, A. *J. Chromatogr. A* **2005**, 1065, 3.

4. Jungbauer, A.; Hahn, R. *J. Chromatogr. A* **2008**, 1184, 62.
5. Mayr, M.; Mayr, B.; Buchmeiser, M. R. *Angew. Chem.* **2001**, *113*, 3957.
6. Mayr, M.; Wang, D.; Kröll, R.; Schuler, N.; Prühs, S.; Fürstner, A.; Buchmeiser, M. R. *Adv. Synth. Catal.* **2005,** 347, 484.
7. Buchmeiser, M. R.; Lubbad, S.; Mayr, M.; Wurst, K. *Inorg. Chim. Acta* **2003**, *345*, 145.
8. Krause, J. O.; Lubbad, S.; Nuyken, O.; Buchmeiser, M. R. *Adv. Synth. Catal.* **2003**, *345*, 996.
9. Krause, J. O.; Lubbad, S. H.; Nuyken, O.; Buchmeiser, M. R. *Macromol. Rapid Commun.* **2003**, *24*, 875.
10. Xie, S.; Švec, F.; Fréchet, J. M. J. *Biotechnol. Bioeng.* **1999**, *62*, 30.
11. Löber, A.; Verch, A.; Schlemmer, B.; Höfer, S.; Frerich, B.; Buchmeiser, M. R. *Angew. Chem.* **2008**, *120*, 9279.
12. Sinner, F.; Buchmeiser, M. R. *Angew. Chem.* **2000**, *112*, 1491.
13. Sinner, F.; Buchmeiser, M. R. *Macromolecules* **2000**, *33*, 5777.
14. Sinner, F. M.; Gatschelhofer, C.; Mautner, A.; Magnes, C.; Buchmeiser, M. R.; Pieber, T. R. *J. Chromatogr. A.* **2008**, 1191, 274.
15. Mayr, B.; Tessadri, R.; Post, E.; Buchmeiser, M. R. *Anal. Chem.* **2001**, *73*, 4071.
16. Buchmeiser, M. R. *Macromol. Rapid. Commun.* **2001**, *22*, 1081.
17. Lubbad, S.; Mayr, B.; Huber, C. G.; Buchmeiser, M. R. *J. Chromatogr. A* **2002**, 959, 121.
18. Lubbad, S.; Buchmeiser, M. R. *Macromol. Rapid Commun.* **2002**, *23*, 617.
19. Mayr, B.; Hölzl, G.; Eder, K.; Buchmeiser, M. R.; Huber, C. G. *Anal. Chem.* **2002**, *74*, 6080.
20. Lubbad, S.; Buchmeiser, M. R. *Macromol. Rapid Commun.* **2003**, *24*, 580.
21. Gatschelhofer, C.; Magnes, C.; Pieber, T. R.; Buchmeiser, M. R.; Sinner, F. M. *J. Chromatogr. A* **2005,** 1090, 81.
22. Lubbad, S.; Steiner, S. A.; Fritz, J. S.; Buchmeiser, M. R. *J. Chromatogr. A* **2006**, 1109, 86.
23. Bandari, R.; Prager-Duschke, A.; Kühnel, C.; Decker, U.; Schlemmer, B.; Buchmeiser, M. R. *Macromolecules* **2006**, *39*, 5222.
24. Schlemmer, B.; Gatschelhofer, G.; Pieber, T. R.; Sinner, F. M.; Buchmeiser, M. R. *J. Chromatogr. A* **2006**, 1132, 124.
25. Sedláková, P.; Miksik, I.; Gatschelhofer, C.; Sinner, F. M.; Buchmeiser, M. R. *Electrophoresis* **2007**, *28*, 2219.
26. Bandari, R.; Knolle, W.; Buchmeiser, M. R. *Macromol. Rapid Commun.* **2007**, *28*, 2090.
27. Bandari, R.; Knolle, W.; Prager-Duschke, A.; Buchmeiser, M. R. *Macromol. Chem. Phys.* **2007,** 208, 1428.
28. Bandari, R.; Knolle, W.; Buchmeiser, M. R. *Macromol. Symp.* **2007**, 254, 87.
29. Bandari, R.; Elsner, C.; Knolle, W.; Kühnel, C.; Decker, U.; Buchmeiser, M. R. *J. Sep. Sci.* **2007,** *30*, 2821.
30. Bandari, R.; Knolle, W.; Buchmeiser, M. R. *J. Chromatogr. A.* **2008**, 1191, 268.
31. Djakovitch, L.; Heise, H.; Köhler, K. *J. Organomet. Chem.* **1999**, 584, 16.
32. Mehnert, C. P.; Ying, J. Y. *Chem. Commun.* **1997**, 2215.
33. Bedford, R. B.; Singh, U. G.; Walton, R. I.; Williams, R. T.; Davis, S. A. *Chem. Mater.* **2005**, *17*, 701.

34. Kwon, M. S.; Kim, N.; Park, C. M.; Lee, J. S.; Kang, K. Y.; Park, J. *Org. Lett.* **2005**, *7*, 1077.
35. Lu, A.-H.; Li, W.-C.; Hou, Z.; Schüth, F. *Chem. Commun.* **2007**, 1038.
36. Niederer, J. P. M.; Arnold, A. B. J.; Hölderich, W. F.; Spliethof, B.; Tesche, B.; Reetz, M.; Bönnemann, H. *Top. Catal.* **2002**, *18*, 265.
37. Oyamada, H.; Akiyama, R.; Hagio, H.; Naito, T.; Kobayashi, S. *Chem. Commun.* **2006**, 4297.
38. Guo, Z.; Henry, L. L.; Palshin, V.; Podlaha, E. J. *J. Mater. Chem.* **2006**, *16*, 1772.
39. Hong, Y.; Sen, A. *Chem. Mater.* **2007**, *19*, 961.
40. De Zan, L.; Gasparovicova, D.; Kralik, M.; Centomo, P.; Carraro, M.; Campestrini, S.; Jerabek, K.; Corain, B. *J. Mol. Cat. A: Chemical* **2007**, *265*, 1.
41. Le Bars, J.; Specht, U.; Bradley, J. S.; Blackmond, D. G. *Langmuir* **1999**, *15*, 7621.
42. Okamoto, K.; Akiyama, R.; Yoshida, H.; Yoshida, T.; Kobayashi, S. *J. Am. Chem. Soc.* **2005**, *127*, 2125.
43. Lu, Y.; Mei, Y.; Drechsler, M.; Ballauff, M. *Angew. Chem.* **2006**, *118*, 827.
44. Dams, M.; Drijkoningen, L.; De Vos, D.; Jacobs, P. *Chem. Commun.* **2002**, 1062.
45. Kiraly, Z.; Veisz, B.; Mastalir, A.; Razga, Z.; Dekani, I. *Chem. Commun.* **1999**, 1925.
46. Aiken III, J. D.; Finke, R. G. *J. Molec. Catal. A: Chem.* **1999**, *145*, 1.
47. Beller, M.; Riermeier, T. H. *Tetrahedron Lett.* **1996**, *37*, 6535.
48. Beller, M.; Fischer, H.; Kühlein, K.; Reisinger, C.-P.; Herrmann, W. A. *J. Organomet. Chem.* **1996**, *520*, 257.
49. Reetz, M. T.; Westermann, E. *Angew. Chem.* **2000**, *112*, 170.
50. Reetz, M. T.; Westermann, E.; Lohmer, R.; Lohmer, G. *Tetrahedron Lett.* **1998**, *39*, 8449.
51. Luo, C.; Zhang, Y.; Wang, Y. *J. Molec. Catal. A: Chem.* **2005**, *229*, 7.
52. Reetz, M. T.; de Vries, J. G. *Chem. Commun.* **2004**, 1559.
53. Caló, V.; Nacci, A.; Monopoli, A.; Detomaso, A.; Iliade, P. *Organometallics* **2003**, *33*, 4193.
54. Rocaboy, C.; Gladysz, J. A. *Org. Lett.* **2002**, *4*, 1993.
55. Reetz, M. T.; Lohmer, G. *Chem. Commun.* **1996**, 1921.
56. Zhao, F.; Shirai, M.; Arai, M. *J. Mol. Catal.: A Chem.* **2000**, *154*, 39.
57. Yao, Q.; Kinney, E. P.; Yang, Z. *J. Org. Chem.* **2003**, *68*, 7528.
58. Arvela, R. K.; Leadbeater, N. E. *J. Org. Chem.* **2005**, *70*, 1786.
59. Hu, J.; Liu, Y. *Langmuir* **2005**, 2121.
60. Liu, Y.; Khemtong, C.; Hu, J. *Chem. Commun.* **2004**, 398.
61. Cassol, C. C.; Umpierre, A. P.; Machado, G.; Wolke, S. I.; Dupont, J. *J. Am. Chem. Soc.* **2005**, *127*, 3298.
62. Li, Y.; Hong, X. M.; Collard, D. M.; El-Sayed, M. A. *Org. Lett.* **2000**, *2*, 2385.
63. Underhill, R. S.; Liu, G. *Chem. Mater.* **2000**, *12*, 3633.
64. Toshima, M.; Shiraishi, Y.; Teranishi, T.; Miyake, M.; Tominaga, T.; Watanabe, H.; Brijoux, W.; Bönnemann, H.; Schmid, G. *Appl. Organomet. Chem.* **2001**, *15*, 178.
65. Shenhar, R.; Norsten, T. B.; Rotello, V. M. *Adv. Mater.* **2005**, *17*, 657.
66. Burda, C.; Chen, X.; Narayanan, R.; A. El-Sayed, M. A. *Chem. Rev.* **2005**, *105*, 1025.
67. Astruc, D.; Lu, F.; Ruiz Aranzaes, J. *Angew. Chem.* **2005**, *117*, 8062.
68. Caló, V.; Nacci, A.; Monopoli, A.; Montingelli, F. *J. Org. Chem.* **2005**, *70*, 6040.

69. Astruc, D. *Inorg. Chem.* **2007**, *46*, 1884.
70. Weck, M.; Jones, C. W. *Inorg. Chem.* **2007**, *46*, 1865.
71. Tsvelikhovsky, D.; Popov, I.; Gutkin, V.; Rozin, A.; Shvartsman, A.; Blum, J. *Eur. J. Org. Chem.* **2008**, 98.
72. Bandari, R.; Höche, T.; Prager, A.; Dirnberger, K.; Buchmeiser, M. R. *Chem . Eur. J.* **2010**, *16*, 4650.
73. Halász, I.; Martin, K. *Angew. Chem.* **1978**, *90*, 954.
74. Švec, F.; Fréchet, J. M. J. *Adv. Mater.* **1994**, *6*, 242.
75. Amatore, C.; Jutand, A. *Acc. Chem. Res.* **2000**, *33*, 314.
76. de Vries, J. G. *Dalton-Trans.* **2006**, 421.
77. Halász, I.; Martin, K. *Ber. Bunsenges. Phys. Chem.* **1975**, *79*, 731.
78. Mayr, B.; Tessadri, R.; Post, E.; Buchmeiser, M. R. *Anal. Chem.* **2001**, *73*, 4071.
79. Buchmeiser, M. R.; Wurst, K. *J. Am. Chem. Soc.* **1999**, *121*, 11101.
80. Martins, C. R.; Ruggeri, G.; Paoli, M.-A. D. *J. Braz. Chem. Soc.* **2003**, *14*, 797.

